INTEGRATION METHODS FOR IMPROVED STABILITY AND ACCURACY OF HYBRID SIMULATIONS

G. Mosqueda[1] and M. Ahmadizadeh[2]

[1] *Assistant Professor, University at Buffalo, the State University of New York, USA*
[2] *Assistant Professor, Department of Civil Engineering, Shiraz University, Shiraz, Iran*
Email: mosqueda@eng.buffalo.edu, ahmadiz@shirazu.ac.ir

ABSTRACT:

Two novel implementation methods of implicit integration procedures for hybrid simulation are presented. The first solves the equation of motion using a fully implicit iterative formulation. The experimental restoring force for each iterative displacement is estimated from curve-fitting of recent force-displacement measurements, avoiding physical iterations on the experimental substructures. For steps that do not converge, the procedure defaults to an explicit formulation. The second integration procedure is a modified operator-splitting integration scheme with two enhancements: a new formulation for the prediction phase with improved accuracy, and the use of an estimated tangent stiffness matrix of the experimental substructure to improve the accuracy of the correction step. A procedure for estimating the experimental tangent stiffness matrix is presented; it is updated only in the steps with significant displacement increments, and remains unchanged otherwise to ensure that the quality of measured data is reliable. Both integration procedures have been successfully implemented experimentally and shown to improve the stability and accuracy of hybrid simulations. Numerical and experimental simulations demonstrate the effectiveness of these integration schemes, especially in utilization of longer time steps, prevention of excitation of higher modes, and testing of stiff and highly nonlinear systems. Improvements in accuracy are demonstrated by measuring the energy balance in the equation of motion.

KEYWORDS: Hybrid simulation, Numerical integration, Implicit integration, Tangent stiffness

1. INTRODUCTION

The path-dependent behavior of experimental specimens does not allow for direct implementations of iterative implicit integration procedures in hybrid simulations. As a result, explicit procedures have been more popular since in these methods, the displacement command for the actuator is directly computed at the beginning of each step. However these methods are conditionally stable and have stringent time step requirements for stiff systems, or systems with high-frequency modes. Extensive research has been dedicated to the development of improved integration algorithms that can be easily applied to hybrid simulations.

A number of improved integration methods utilize implicit formulations by introducing feedback loops involving single-degree-of-freedom (SDF) experimental substructures (Thewalt and Mahin 1987; Shing *et al.* 1991; Shing *et al.* 2006). These procedures have onerous communication requirements between experimental and numerical substructures, and require specialized control strategies to avoid unwanted displacement reversals during iterations on experimental substructures. In order to address these issues, other integration methods have been introduced that apply implicit iterations only in numerical substructure (Schneider and Roeder 1994; Ghaboussi *et al.* 2006), or use the initial elastic stiffness matrix of the experimental substructure to approximate its behavior (Nakashima *et al.* 1990; Zhang *et al.* 2005; Chang and Sung 2006; Wu *et al.* 2006). The initial stiffness approximation is reasonable for mildly nonlinear systems, when an experimental tangent stiffness matrix may be difficult to estimate. Estimation of tangent stiffness of the experimental substructures has also been attempted in hybrid simulations. These stiffness matrices have been used for error computations (Thewalt

and Roman 1994), delay compensation (Carrion and Spencer 2006) and establishing an instantaneous force-displacement relation for SDF experimental substructures (Pan *et al.* 2005).

In this paper, new integration procedures are proposed for displacement-controlled hybrid simulations. In one method, recent measurements are used to estimate restoring forces in an iterative scheme to satisfy the implicit formulation of the equation of motion. In the other method, an experimental tangent stiffness matrix is updated in each integration step using measurements, and then used in the operator-splitting solution procedure to improve the correction step. The effectiveness of these methods is demonstrated through hybrid simulations, including a two-degree-of-freedom experimental substructure and a series of numerical simulations.

2. HYBRID SIMULATION

In a hybrid simulation, the equation of motion of the combined numerical and experimental structural model can be expressed as:

$$\mathbf{Ma} + \mathbf{Cv} + \mathbf{Kd} + \mathbf{r} = -\mathbf{M}^{\mathrm{t}}\boldsymbol{\iota}\ddot{u}_g \tag{2.1}$$

in which $\mathbf{M}$, $\mathbf{C}$ and $\mathbf{K}$ are mass, damping, and stiffness matrix of the numerical substructure, $\mathbf{M}^{\mathrm{t}}$ is the total mass matrix (including experimental mass) of the structural model, $\boldsymbol{\iota}$ is the influence vector, $\mathbf{d}$, $\mathbf{v}$, and $\mathbf{a}$ are displacement, velocity and acceleration vectors, respectively; $\ddot{u}_g$ is the input ground acceleration and $\mathbf{r}$ is the restoring force measured in the experimental substructures. The experimental restoring force vector may include strain-dependent, damping, or inertial forces. In this study, the experimental substructures are assumed to be mainly strain-dependent.

3. INTEGRATION ALGORITHM

The formulation of α-method by Hilber *et al.* (1977) used in the proposed integration algorithms is presented in this section. In the α-method, the time-discrete equation of motion and finite difference relations for determination of displacement and velocity at step n are given by:

$$\mathbf{Ma}_n + \mathbf{Cv}_n + \mathbf{Kd}_n + \alpha\left[\mathbf{C}\left(\mathbf{v}_n - \mathbf{v}_{n-1}\right) + \mathbf{K}\left(\mathbf{d}_n - \mathbf{d}_{n-1}\right)\right] = -\mathbf{M}^{\mathrm{t}}\boldsymbol{\iota}\ddot{u}_g\left(t_n + \alpha\Delta t\right) \tag{3.1}$$

$$\mathbf{d}_n = \mathbf{d}_{n-1} + \Delta t\mathbf{v}_{n-1} + \Delta t^2\left[\left(1/2 - \beta\right)\mathbf{a}_{n-1} + \beta\mathbf{a}_n\right] \tag{3.2}$$

$$\mathbf{v}_n = \mathbf{v}_{n-1} + \Delta t\left[\left(1-\gamma\right)\mathbf{a}_{n-1} + \gamma\mathbf{a}_n\right] \tag{3.3}$$

in which Δt is the integration time step. This method provides numerical energy dissipation controllable by the parameter α. If the parameters are selected such that $-1/3 \le \alpha \le 0$, $\gamma = \left(1-2\alpha\right)/2$, and $\beta = \left(1-\alpha\right)^2/4$, an unconditionally stable, second-order accurate scheme results.

In a hybrid simulation, Eq. (3.1) should be modified to include the restoring force vector from the experimental substructure:

$$\begin{aligned}&\mathbf{Ma}_n + \mathbf{Cv}_n + \mathbf{Kd}_n + \mathbf{r}_n + \\ &\alpha\left[\mathbf{C}\left(\mathbf{v}_n - \mathbf{v}_{n-1}\right) + \mathbf{K}\left(\mathbf{d}_n - \mathbf{d}_{n-1}\right) + \mathbf{r}_n - \mathbf{r}_{n-1} - \mathbf{M}^{\mathrm{e}}\left(\mathbf{a}_n - \mathbf{a}_{n-1}\right)\right] = -\mathbf{M}^{\mathrm{t}}\boldsymbol{\iota}\ddot{u}_g\left(t_n + \alpha\Delta t\right)\end{aligned} \tag{3.4}$$

where $\mathbf{M}^{\mathrm{e}} = \mathbf{M}^{\mathrm{t}} - \mathbf{M}$ is the experimental mass matrix. In a fast pseudo-dynamic test, the inertial mass effect should be removed from the incremental feedback force vector in Eq. (3.4), so that the remainder will only include strain-dependent and damping effects.

In a conventional operator-splitting integration method, the predictor displacement normally includes only the explicit portion of Eq. (3.2); that is, the predictor displacement is given by $\tilde{\mathbf{d}}_n = \mathbf{d}_{n-1} + \Delta t\mathbf{v}_{n-1} + \Delta t^2\left(1/2 - \beta\right)\mathbf{a}_{n-1}$.

The corrector step will then add $\beta\Delta t^2\mathbf{a}_n$ to the predictor displacement to satisfy Eq. (3.2). In this study, Eq. (3.2) is used in explicit form by temporarily setting $\beta = 0$ to calculate the predictor displacement:

$$\tilde{\mathbf{d}}_n = \mathbf{d}_{n-1} + \Delta t\mathbf{v}_{n-1} + \frac{1}{2}\Delta t^2\mathbf{a}_{n-1} \tag{3.5}$$

The displacements applied on the experimental substructure are determined by a transformation to the actuator local coordinate system using $\tilde{\mathbf{d}}_n^l = \mathbf{T}\tilde{\mathbf{d}}_n$, where $\mathbf{T}$ is the displacement transformation matrix. The imposition of these displacements will result in the predictor measured force vector in actuator coordinate system, $\tilde{\mathbf{r}}_n^l$. After the corrector step, the final (converged) displacement vector (which satisfies the implicit formulation) will be:

$$\mathbf{d}_n = \tilde{\mathbf{d}}_n + \beta\Delta t^2\left(\mathbf{a}_n - \mathbf{a}_{n-1}\right) \tag{3.6}$$

Note that the correction term $\beta\Delta t^2\left(\mathbf{a}_n - \mathbf{a}_{n-1}\right)$ is normally smaller than $\beta\Delta t^2\mathbf{a}_n$ used in the original operator-splitting formulation, thus providing more accurate predictor displacements. In this study, two integration algorithms are introduced that apply an explicit displacement (Eq. (3.5)) in each step, and then update the states according to the change in the displacement vector given by Eq. (3.6).

4. FULLY IMPLICIT INTEGRATION FOR HYBRID SIMULATION

The major challenge in implementing implicit integration algorithms in a hybrid simulation is that iterative displacement reversals may result in unrecoverable damage to experimental specimens or erroneous energy dissipation. Therefore, it is not advisable to measure experimental restoring forces, $\mathbf{r}_n^i$, by physically imposing the iterative displacements. In the proposed fully implicit integration method, recent experimental measurements are used to capture the instantaneous behavior of experimental substructures and estimate forces corresponding to iterative displacements.

The iterations are implemented numerically, without physical imposition of iterative displacements on the experimental substructures using the following procedure. First, the actuator command displacements are predicted using an explicit expression (Eq. (3.5)) to load the experimental substructures. Second, the displacements and forces measured through the load path are used in the iterative scheme to satisfy an implicit formulation, given by Eqs. (3.2)-(3.4). Next, force estimation procedure for iterative displacements is followed using the recent measurements. Second-order polynomials are fitted to both measured displacement and force histories in local actuator coordinates. In this procedure, the trial displacements are determined in actuator coordinate system in each iteration, but they are not physically imposed on the specimen. Instead, the fitted polynomials are used to estimate forces corresponding to each of the iterative displacements by using time stamps as a parameter relating force and displacement polynomials, as shown in Figure 1. The iterative procedure is repeated until a convergence criterion is satisfied, such as:

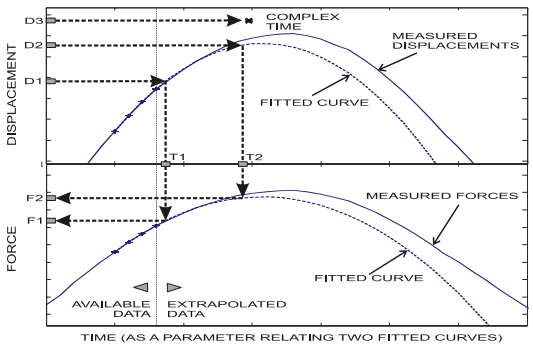

Figure 1 Estimation of force corresponding to the desired displacement using measurements.

$$\frac{\left\|\mathbf{d}_n^i - \mathbf{d}_n^{i-1}\right\|}{\left\|\mathbf{d}_n^i\right\|} < \varepsilon \tag{4.1}$$

where ε is the convergence tolerance for the normalized displacement increment, and superscripts denote the iteration number.

As with most iterative integration schemes for non-linear systems, convergence cannot be guaranteed in each step, especially for a hybrid simulation that also involves experimental errors. The failed integration steps can be identified by detection of excessive time parameter variation, or convergence failure after maximum number of iterations. An alternate solution strategy is necessary for the simulation to continue in case the iterative solution scheme fails. Here, it is proposed to revert to an explicit procedure by selecting the displacement of Eq. (3.5) as the final solution for the step. The measured restoring force vector $\mathbf{r}_n$ is then directly used to determine acceleration and velocity vectors at step n using Eq. (3.3) and:

$$\mathbf{a}_n = \mathbf{A}^{-1}\left\{\begin{array}{l}\mathbf{M}^{\mathrm{t}}\boldsymbol{\iota}\ddot{u}_g\left(t_n+\alpha\Delta t\right)\\ -\left[\mathbf{C}\left(\mathbf{v}_{n-1}+\left(1+\alpha\right)\dfrac{\Delta t}{2}\mathbf{a}_{n-1}\right)+\left(1+\alpha\right)\left(\mathbf{K}\mathbf{d}_n+\mathbf{r}_n\right)+\alpha\left(\mathbf{M}^{\mathrm{e}}\mathbf{a}_{n-1}-\mathbf{K}\mathbf{d}_{n-1}-\mathbf{r}_{n-1}\right)\right]\end{array}\right\} \tag{4.2}$$

where

$$\mathbf{A}=\mathbf{M}+\left(1+\alpha\right)\frac{\Delta t}{2}\mathbf{C}-\alpha\mathbf{M}^{\mathrm{e}} \tag{4.3}$$

If the initial stiffness matrix of the system is available, an operator-splitting method can also be utilized in the steps with failed implicit iterations to update the state vectors.

5. OPERATOR-SPLITTING INTEGRATION WITH ESTIMATION OF EXPERIMENTAL STIFFNESS MATRIX

The integration method proposed in this section takes advantage of measurements to update a condensed experimental tangent stiffness matrix. The tangent stiffness is then used in an operator-splitting method to improve its accuracy for testing nonlinear systems. Following a procedure similar to the previous section, the predictor displacement of Eq. (3.5) is applied on the experimental substructure and the restoring force is measured. In the corrector step, Eq. (3.6) is used to update the displacement vector. As a result of this change in displacement vector, force vector $\tilde{\mathbf{r}}_n^l$ should also be updated in the corrector step:

$$\mathbf{r}_n^l=\tilde{\mathbf{r}}_n^l+\mathbf{K}_n^l\left(\mathbf{d}_n^l-\tilde{\mathbf{d}}_n^{l,m}\right) \tag{5.1}$$

where $\mathbf{d}_n^l$ is the displacement vector given by Eq. (3.6), $\tilde{\mathbf{d}}_n^{l,m}$ is the measured displacement vector, and $\mathbf{K}_n^l$ is the experimental stiffness matrix at step n, all expressed in the actuator coordinate system. Note that in a conventional operator-splitting method, $\mathbf{K}_n^l$ is simply the initial experimental stiffness matrix. By using the measured displacement vector $\tilde{\mathbf{d}}_n^{l,m}$, Eq. (5.1) not only updates the force vector due to displacement modification of Eq. (3.6), but also attempts to correct for actuator tracking errors. The corrected restoring force vector is then transformed to the global coordinate system using $\mathbf{r}_n=\mathbf{T}^T\mathbf{r}_n^l$, and used in the combination of Eqs. (3.3), (3.4), (3.6) and (5.1) to update the states.

For use in this procedure, an experimental tangent stiffness matrix is estimated that satisfies the following incremental force-displacement relation at the n^{th} integration step:

$$\Delta\mathbf{r}_n^l=\mathbf{K}_n^l\Delta\mathbf{x}_n^l \tag{5.2}$$

where $\Delta\mathbf{r}_n^l$ and $\Delta\mathbf{x}_n^l$ are incremental force and displacement vectors of the experimental substructure in actuator local coordinate system, respectively, and $\mathbf{K}_n^l$ is the $m\times m$ stiffness matrix of the experimental substructure, m being the number of actuators (and load cells).

The conventional static test sequence for estimation of experimental stiffness matrix cannot be applied to online hybrid simulations. The required procedures should estimate the tangent stiffness only using $m\times 1$ vectors of measured force and displacement data. In the proposed procedure, some information about the physical test

system and experimental element configuration is first used to reduce the number of unknowns required to update the tangent stiffness matrix.

A brief look at structural analysis problems reveals that the stiffness matrices of most structural elements consist of terms that are a combination of a few geometric and material properties. From a macroscopic standpoint, similar intrinsic parameters often exist that determine the resistance of a structure to loads imposed by actuators. For example, the lateral stiffness of a bracing system subjected to horizontal displacements provides a sufficient force-displacement relation, regardless of the configuration of individual elements. As another example, the entire $N \times N$ stiffness matrix of an N-story shear building can be found from N story stiffnesses. Hence, by considering only the key intrinsic parameters, the stiffness matrix $\mathbf{K}_n^l$ of the experimental substructure in the actuator coordinate system can often be expressed as:

$$\mathbf{K}_n^l = \mathbf{T}_p^T \mathbf{P}_n \mathbf{T}_p \tag{5.3}$$

where $\mathbf{P}_n$ is a diagonal $p \times p$ matrix of essential stiffness parameters. The transformation matrix $\mathbf{T}_p$ transform displacements from the local actuator (substructure) coordinate system to an intrinsic (parameter) coordinate system with a presumed diagonal stiffness matrix $\mathbf{P}_n$. For the example of shear building, $\mathbf{P}_n$ is a diagonal matrix of story stiffness, and $\mathbf{T}_p$ simply transforms the displacements to story drifts.

In order to calculate the terms of the diagonal stiffness matrix $\mathbf{P}_n$, the incremental displacement and force vectors should be transformed to the above-mentioned intrinsic coordinate system. For displacements, the transformation can be carried out through the same transformation matrix described above:

$$\Delta \mathbf{x}_n^p = \mathbf{T}_p \Delta \mathbf{x}_n^l \tag{5.4}$$

in which $\Delta \mathbf{x}_n^l$ and $\Delta \mathbf{x}_n^p$ are the displacement increment vectors in actuator and intrinsic coordinate systems, respectively. The transformation of displacements from global to actuator coordinate system can be carried out using $\Delta \mathbf{x}_n^l = \mathbf{T} \Delta \mathbf{x}_n$.

For statically determinate structures, the intrinsic forces can simply be found by equilibrium, and the transformation of local incremental force vector $\Delta \mathbf{r}_n^l$ to intrinsic coordinates ($\Delta \mathbf{r}_n^p$) is:

$$\Delta \mathbf{r}_n^p = \mathbf{T}_p^{(-T)} \Delta \mathbf{r}_n^l \tag{5.5}$$

where the superscript $(-T)$ represents a pseudo-inverse of the matrix transpose. If the experimental substructure is statically indeterminate, the calculation of forces in intrinsic coordinates requires the stiffness matrix of the system for a structural analysis. In this case, the structure should be analyzed to find local displacements from the measured local force vector, $\Delta \mathbf{r}_n^l$. The resulting local displacements can then be transformed to the intrinsic coordinate system using Eq. (5.4). The intrinsic forces will be the forces corresponding to the intrinsic displacement vector using diagonal stiffness matrix $\mathbf{P}_n$:

$$\Delta \mathbf{r}_n^p = \mathbf{P}_n \mathbf{T}_p \left(\mathbf{K}_n^l \right)^{-1} \Delta \mathbf{r}_n^l \tag{5.6}$$

Note that to omit the iterative procedure involved in the use of the above equation, it can be approximately replaced by $\Delta \mathbf{r}_n^p = \mathbf{P}_{n-1} \mathbf{T}_p \left(\mathbf{K}_{n-1}^l \right)^{-1} \Delta \mathbf{r}_n^l$, updated once at the beginning of each integration step. After determination of forces and displacements in the intrinsic coordinate system, each diagonal element of the updated parameter matrix can be found by dividing the corresponding elements of force vector by the displacement vector. Put in matrix form, the expression will be:

$$\mathbf{P}_n = \mathrm{diag}\left(\Delta \mathbf{x}_n^p \right)^{-1} \mathrm{diag}\left(\Delta \mathbf{r}_n^p \right) \tag{5.7}$$

The global stiffness matrix of the experimental substructures can then be found using:

$$\mathbf{K}_n = \mathbf{T}^T \mathbf{K}_n^l \mathbf{T} \tag{5.8}$$

The fidelity of displacement and force measurements used in Eq. (5.7) is essential to the accuracy of the estimated stiffness matrix. Hence, it is important to minimize the amount of noise in the measured force and displacement vectors. For this purpose, it is suggested to update the stiffness matrix only in integration steps with displacement increments sufficiently larger than the noise level. For example, the incremental displacement vector should satisfy:

$$\left\| \Delta \mathbf{x}_n^l \right\|_\infty > \delta \tag{5.9}$$

where $\left\| \Delta \mathbf{x}_n^l \right\|_\infty$ denotes the largest element of the absolute incremental displacement vector, and δ is displacement increment threshold. The displacement threshold δ should be greater than the measurement noise level, but small enough to capture steps with significant displacement increments. Pretest simulations with zero input excitation can be used to determine the root-mean-square (RMS) of the noise signal in displacement and force measurements. Recommended value of ε is the greater of: 10 times the RMS of displacement noise or a value that results in a force (using initial stiffness) 10 times greater than the RMS of force noise.

6. EXPERIMENTAL VERIFICATIONS

The two-story structure shown in Figure 2 is considered for the experimental verification of the proposed integration methods. The entire stiffness of the hybrid model is represented by a two-degree-of-freedom experimental substructure. Damping is numerically modeled to be 5% of critical in the first mode. The response of the structure subjected to the 1978 Tabas earthquake (a near-fault record with a peak ground acceleration of 0.85g) is simulated at the real-time event scale with integration time step of 10/1024 seconds.

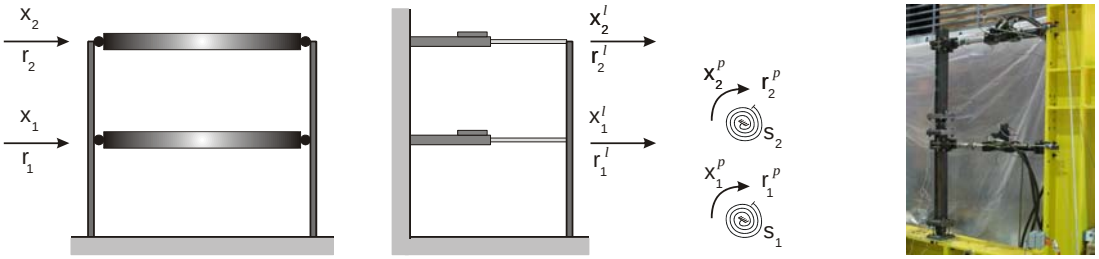

Figure 2 Two-degree-of-freedom structure, corresponding laboratory setup for experimental substructure column, and stiffness components in the intrinsic coordinate system.

Based on the measured initial stiffness of the experimental substructure, a mass matrix is selected to attain natural periods of 0.50 and 0.13 seconds. For comparison purposes, and to keep the specimens in linear range, two simulations with 2.5% excitation amplitude scale have been carried out using an explicit method and the proposed fully implicit integration procedure. As illustrated in Figure 3, although the simulation is within the stability limit of the explicit integration procedure, it becomes unstable due to the presence of experimental errors. The proposed integration method with implicit or explicit steps (with 68.8% successful implicit steps), however, remains stable and accurate throughout the simulation. The effectiveness of this test procedure has also been verified in nonlinear systems (Mosqueda and Ahmadizadeh 2007).

In another simulation, the mass matrix is modified to obtain periods of 0.6 and 0.15 seconds, and the excitation amplitude scale is increased to 35% to increase the internal forces and result in a nonlinear response. The simulation results using operator-splitting method with experimental tangent stiffness are shown in Figure 4. As illustrated, the response is nonlinear, and residual drifts of 14 and 28 millimeters can be observed in the first and second stories, respectively. In this experimental simulation, the stiffness matrix was updated in 64.0% of the integration steps (85.3% for the period of significant response between 5 and 30 seconds). In other steps, the displacement norm was less than the noise threshold (0.1mm). The terms of the experimental stiffness matrix through the simulation are shown in Figure 4(b). The estimated stiffness matrix appears to have a fair amount of

noise, which can be reduced by improved filtering of the measurements. Even so, this estimate is sufficient to improve the accuracy compared to the conventional operator-splitting approach.

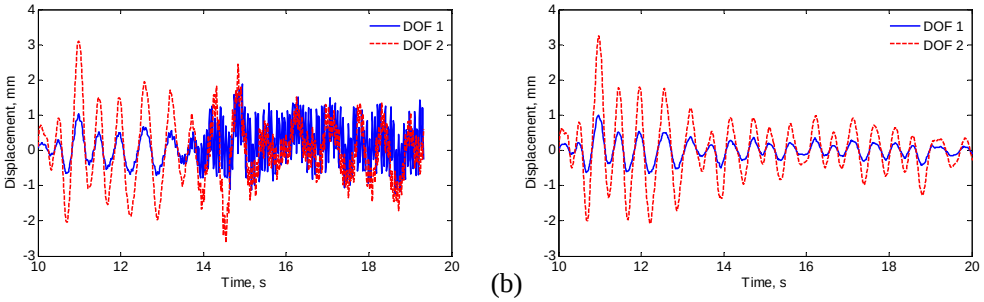

Figure 3 Displacement history of linear experimental simulations of two-degree-of-freedom system – (a) explicit central difference, and (b) combined implicit or explicit integration.

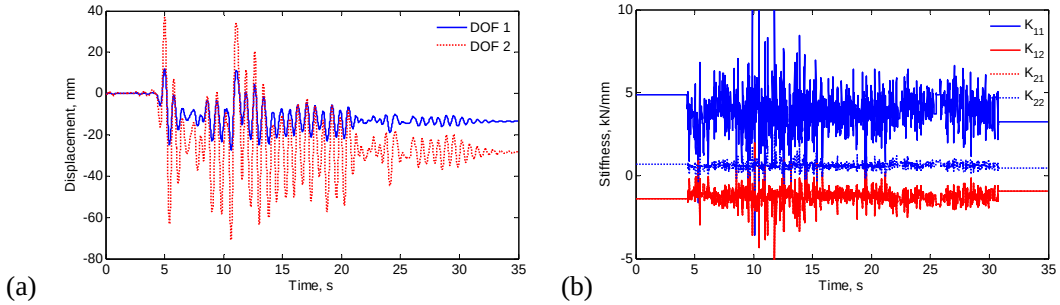

Figure 4 (a) Displacement history of a nonlinear simulation with 35% Tabas earthquake, and (b) stiffness matrix elements during the simulation.

The energy balance of the system is well maintained throughout the simulation, as shown in Figure 5. The sum of analytical and experimental energies shows an excellent agreement with the input energy. Note that the simulation model does not have any numerical stiffness and numerical strain energy is zero throughout the simulation. The final energy balance error is less than 0.02% of input energy, which is very small. A similar experiment using a constant initial stiffness matrix for experimental substructure (conventional operator-splitting method), shows about 0.45% energy error at the end of simulation. This difference is small for this test structure, due to the fact that the amount of yielding is limited in the present experimental setup by the available actuator stroke. This improvement has been observed to be larger in simulations with highly nonlinear experimental substructures (Ahmadizadeh and Mosqueda 2008).

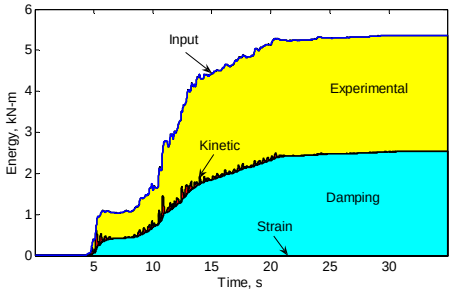

Figure 5 Energy histories computed through the hybrid simulation.

7. CONCLUSIONS

Two new integration procedures have been proposed based on the use of measurements in iterations and estimation of tangent stiffness matrix of the experimental substructure during hybrid simulations. An iterative integration method was proposed that captures the instantaneous behavior of the experimental substructures by using the most recent measurements to satisfy an implicit formulation in a majority of the integration steps. As convergence cannot be guaranteed in nonlinear hybrid simulations with experimental errors, in cases where accurate estimation of forces corresponding to iterative displacements is not possible and convergence fails, the procedure reverts to an explicit or operator-splitting scheme to ensure completion of the integration step. It was shown that this integration method is able to eliminate spurious excitation of high-frequency modes and remain stable using longer time steps compared to explicit methods.

In another integration procedure, the tangent stiffness matrix of the experimental substructure is updated in each integration step following the operator-splitting scheme. In this approach, necessary parameters are first identified and updated during the simulation using the incremental force and displacement vectors. Only significant force-displacement pairs are used to update these parameters; steps with small displacement increments are ignored. The estimated stiffness parameters can then be used to determine reduced experimental stiffness matrix through a simple coordinate system transformation. It was demonstrated that the use of the updated stiffness matrix improves the accuracy of the simulation by reducing the overall energy balance errors.

By using the recent series of measurements in the force and stiffness estimation procedure, the proposed integration methods better capture the actual behavior of experimental setup. In addition, these procedures reduce the required communications between numerical and experimental subsystems, as the exchange of command displacements and acquisition of measurements occur only once within each integration step. These features make the proposed integration algorithms appealing for real-time testing stiff or highly nonlinear systems or applications to geographically distributed experiments.

ACKNOWLEDMENTS

This research was partially supported by the National Science Foundation under grant CMMI-0748111 and through NEES shared use under access under grant CMS-0402490. This support is gratefully acknowledged. The opinions expressed in this paper are those of the authors and do not represent the view of the sponsor.

REFERENCES

Ahmadizadeh, M. and Mosqueda, G. (2008). Hybrid simulation with improved operator-splitting integration using experimental tangent stiffness matrix estimation. *Journal of Structural Engineering*, in press.

Carrion, J.E. and Spencer, B.F. (2006). Real-time hybrid testing using model-based delay compensation. 4th International Conference on Earthquake Engineering, Taipei, Taiwan.

Chang, S.Y. and Sung, Y.C. (2006). An enhanced explicit pseudodynamic algorithm with unconditional stability. 8th National Conference on Earthquake Engineering, San Francisco, CA.

Ghaboussi, J., Yun, G.J. and Hashash, Y.M.A. (2006). A novel predictor-corrector algorithm for sub-structure pseudo-dynamic testing. *Earthquake Engineering & Structural Dynamics* **35:4**, 453-476.

Hilber, H.M., Hughes, T.J.R. and Taylor, R.L. (1977). Improved numerical dissipation for time integration algorithms in structural dynamics. *Earthquake Engineering & Structural Dynamics* **5**, 283-292.

Mosqueda, G. and Ahmadizadeh, M. (2007). Combined implicit or explicit integration steps for hybrid simulation. *Earthquake Engineering & Structural Dynamics* **36:15**, 2325-2343.

Nakashima, M., Kaminoso, T., Ishida, M. and Kazuhiro, A. (1990). Integration techniques for substructure online test. 4th US National Conference of Earthquake Engineering, Palm Springs, CA, Earthquake Engineering Research Institute.

Pan, P., Tada, M. and Nakashima, M. (2005). Online hybrid test by internet linkage of distributed test-analysis domains. *Earthquake Engineering & Structural Dynamics* **34:11**, 1407-1425.

Schneider, S.P. and Roeder, C.W. (1994). An inelastic substructure technique for the pseudodynamic test method. *Earthquake Engineering & Structural Dynamics* **23**, 761-775.

Shing, P.B., Stavridis, A., Wei, Z., Stauffer, E., Wallen, R. and Jung, R.Y. (2006). Validation of a fast hybrid test system with substructure tests. 17th Analysis and Computation Specialty Conference, St. Louis.

Shing, P.S.B., Vannan, M.T. and Cater, E. (1991). Implicit time integration for pseudodynamic tests. *Earthquake Engineering & Structural Dynamics* **20:6**, 551-576.

Thewalt, C.R. and Mahin, S.A. (1987). Hybrid solution techniques for generalized pseudodynamic testing. Berkeley, University of California, Berkeley**:** 133.

Thewalt, C.R. and Roman, M. (1994). Performance parameters for pseudodynamic tests. *Journal of Structural Engineering -- ASCE* **120:9**, 2768-2781.

Wu, B., Xu, G., Wang, Q. and Williams, M.S. (2006). Operator-splitting method for real-time substructure testing. *Earthquake Engineering & Structural Dynamics* **35:3**, 293-314.

Zhang, Y.F., Sause, R., Ricles, J.M. and Naito, C.J. (2005). Modified predictor-corrector numerical scheme for real-time pseudo dynamic tests using state-space formulation. *Earthquake Engineering & Structural Dynamics* **34:3**, 271-288.